

Yearly Report for NASA PIDDP Grant NAG5-8515 (SwRI 15-02992), March 31, 2001

Laboratory Experimentation Model of the 270 Degree Electron Tophat Analyzer by

R. A. Frahm, J. R. Sharber, R. Link, and J. D. Winningham

1. Introduction

One of the most important space plasma measurements is that of a well-resolved low-energy (~ 1 eV to 1 keV) electron spectrum. This range includes the regime where photoelectron and Auger processes are important [Winningham *et al.*, 1989] as well as the very low energy range (down to 1 eV) where electron distributions of temperature 11,000° K are measurable. Knowledge of the structure (\sim eV scale) of the photoelectron spectrum can provide information on the composition of a planetary or cometary atmosphere. As evidence, scientists developing the Analyzer of Space Plasma and Energetic Atoms (ASPERA-3) Electron Spectrometer (ELS) flying on the European Space Agency (ESA) Mars Express Mission have adapted their electron instrument to increase energy resolution in the photoelectron energy region as a means of remotely sensing the Martian atmosphere; the idea being that the Martian magnetic field is so weak that electron interaction between the source and point of detection is non-existent; the measured electrons are therefore reflective of the processes occurring in the Martian atmosphere.

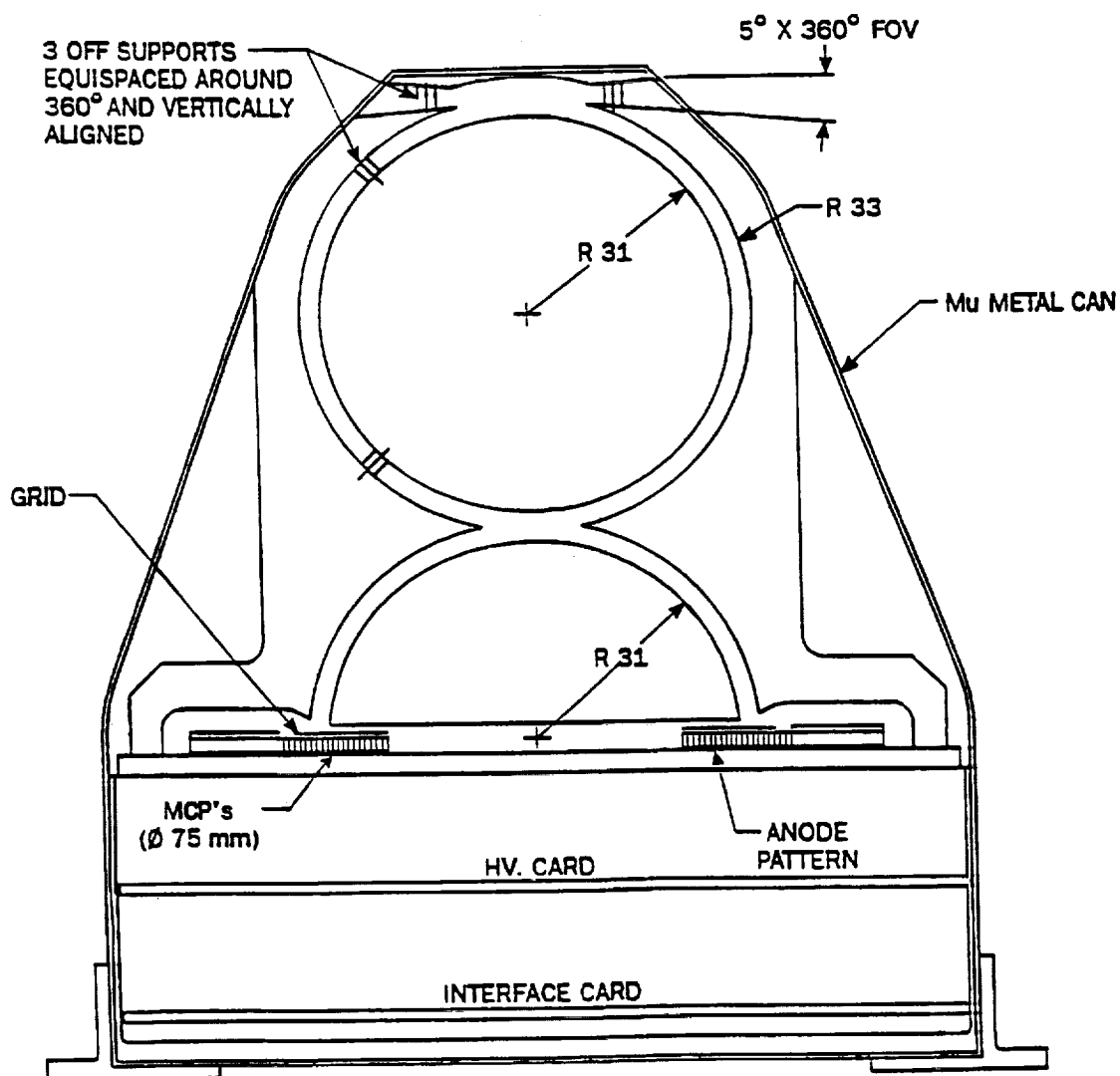
2. Objectives

Our overall objective is to develop an instrument capable of making accurate, high-resolution measurements of electrons over the energy range 1 eV to 1 keV. Specifically, the instrument (the 270° Tophat Analyzer) will have the following properties: a sharp energy resolution ($\Delta E/E \sim 4\%$), sufficient for resolving structure in the photoelectron spectrum; a large geometric factor; excellent Ultraviolet (UV) rejection; significantly reduced mass; and the capability, through the use of passive magnetic shielding, to operate at very low energies. *It thus represents a significant improvement in the measurement technology of this important region of the electron spectrum.*

3. Accomplishments

Figure 1 from the original proposal shows the concept drawing of the 270° Electron Tophat Analyzer and Table 1 show the instrument characteristics as designed. The instrument electrical and mechanical designs were completed. A solution to mechanically mounting the upper sphere and electrically connecting to that sphere as discussed in the previous report has been implemented. The previous report showed the mechanical assembly as an implementation of the design shown in Figure 1. In this report, each section has been expanded to show the internals of the laboratory experimentation model. Figure 2 shows the upper portion of the sensor head. The (upper) spherical deflection plate is hollow and suspended at its equator. The upper housing and lower housing separate for ease of assembly. Electrical connection to the sphere is made through one standoff and the other three standoffs are hollow for outgassing purposes. The sphere is hollow and electrical connections are made at the top and bottom of the sphere to ensure firm electrical contact. The top of the mu-metal shield covers the deflection section.

The reason for moving the location of the sphere's standoffs is that there is less influence to particle trajectories. When electrons travel through the analyzer, they do so on great circle paths. Electrons entering at opposite extremes of the entrance aperture follow great circle paths which meet at a focal point at the equator of the sphere. Thus, the influence of the standoffs at the equator effects only those electrons which come from the particular direction which focuses at the standoff location. If the standoffs were left as designed (Figure 1), their influence would be to block portions of the electrons from a large number of locations, causing influence over a



NOTE: ALL DIMENSIONS IN MILLIMETERS

Figure 1. Cross-section of the 270° Electron Tophat Analyzer.

Table 1: Instrument Characteristics

Description	Value	Description	Value
Geometric Factor per pixel	$3.7 \times 10^{-3} \text{ cm}^2 \text{ sr}$	Energy Resolution	5.7 %
Full Field-of-View planar	5° elevation x 360° azimuth	Radii	31 mm, 33 mm, 35 mm
Pixel Field-of-View planar	5° elevation x 30° azimuth	Mass	approximately 2 kg
Energy Range	approximately 5 eV — 2 keV	Power	approximately 2 Watts
Number of Angular Sectors	12	Accumulation Time	Adjustable

larger portion of the incoming electron paths.

The lower deflection system and sensor section are shown in Figure 3. The hemispherical deflection plate is held in place by the a bottom cup, which contains the anode-microchannel plate detection system. Holes in the base of the cup allow pickoff of signals by the electronics. Mechanical alignment between upper and lower deflection system is produced by the cup. The appropriate distances for the deflection grid, microchannel plate (MCP) stack, and anode grid are also maintained by the cup design.

To minimize magnetic field influence, the cup is surrounded by mu-metal shield. This part of the shield attaches to the upper portion of the mu-metal shield which covers the area shown in Figure 2. The mu-metal shield covers as much of the deflection and sensor system as possible. This scheme should reduce external magnetic field effects from influencing electron trajectories while traversing the 270° deflection path. Of particular concern are magnetic components used in space flight power supply designs since they can be very close to the sensor head. Although this program concentrates on the sensor design and not the flight power system, its presence should be considered.

In order to generate and receive output signals, an electronics system had to be created. The electronics is housed in an electronics box. The analyzer head sits on top of this electronics box. The electronics box is shown in Figure 4. There are two boards in the electronics box. The upper board contains the spring loaded connectors for making contact with the anode system shown in Figure 3. On this board are the amplifiers for the deflection system. Each anode is discrete and each anode signal had its own electronic signal path. The amplification system used discrete amplifiers which kept each anode signal separated as much as possible in order to avoid any electronic noise difficulties. This was desired since the design of a flight electronic system was not the goal of this program and a laboratory setting allowed the use of more power and mass than would be available in a flight system, making the job of signal recovery much easier.

Also unique to a laboratory setting is the lower electronics board. This board contains line drivers for driving signals long distances through the testing systems. Testing facilities are large and a low powered flight system designed to drive short distances on a spacecraft can cause difficulties detecting proper signals in a laboratory setting. Even though a driver system is needed to output signals from the 270° top hat for the laboratory environment, standard laboratory power supplies were used to control the instrument and their design did not need to be included in this work (as proposed).

The assembled laboratory unit is shown in a cut away view in Figure 5. The sensor system is separate from the electronics system. For a flight system, the electronics box would be replaced with one designed for the particular mission. It would contain electronics to detect the anode signal at a minimum, but could contain power supplies, a data processing unit, or an instrument controller, as examples.

The 270° laboratory model outputs signal from 12 sectors, simultaneously. The laboratory counting system monitored one output channel at a time. This system proved cumbersome and very time consuming to use. Signal output would need to be switched to each of the 12 output channels of the 270° instrument for every measurement in order to determine what was happening on each anode. This became unbarable quickly, and we found it easier and more cost effective to construct a separate accumulator to detect all 12 anode outputs, simultaneously.

Testing began on the MCP and counting system. A source of UV was used to flood the MCP with light. This source should cause the MCP to output a uniform signal and each of the anode outputs should be the same. For this test, the deflection system was removed; however, the grid system was included. It was anticipated that there should be a small decrease in counts for those anodes closest to a screen support post. Figure 6 resulted from this test. Major decreases in amplitude were detected in this test. Dips in signal strength occurred in anodes 3, 6, 9, and 12. On inspection, it was discovered that there was a mismatch between the placement of standoffs within the deflection system and the anode pattern. The result was a half anode azimuthal shift. Examination of the costs associated with a correction showed that there were not the funds in this program to solve the design flaw, so it was not corrected. Thus, all results will show strong influences for the four output channels which contain support posts within the path of the particles.

A background test was also performed at this time. For this test, the analyzer is blinded so that there is no input signal. Ideally, the results of this test should show no counts; however, Figure 7 shows that there are self generated counts by the MCP. The MCPs purchased for the 270° laboratory model were not screened by the

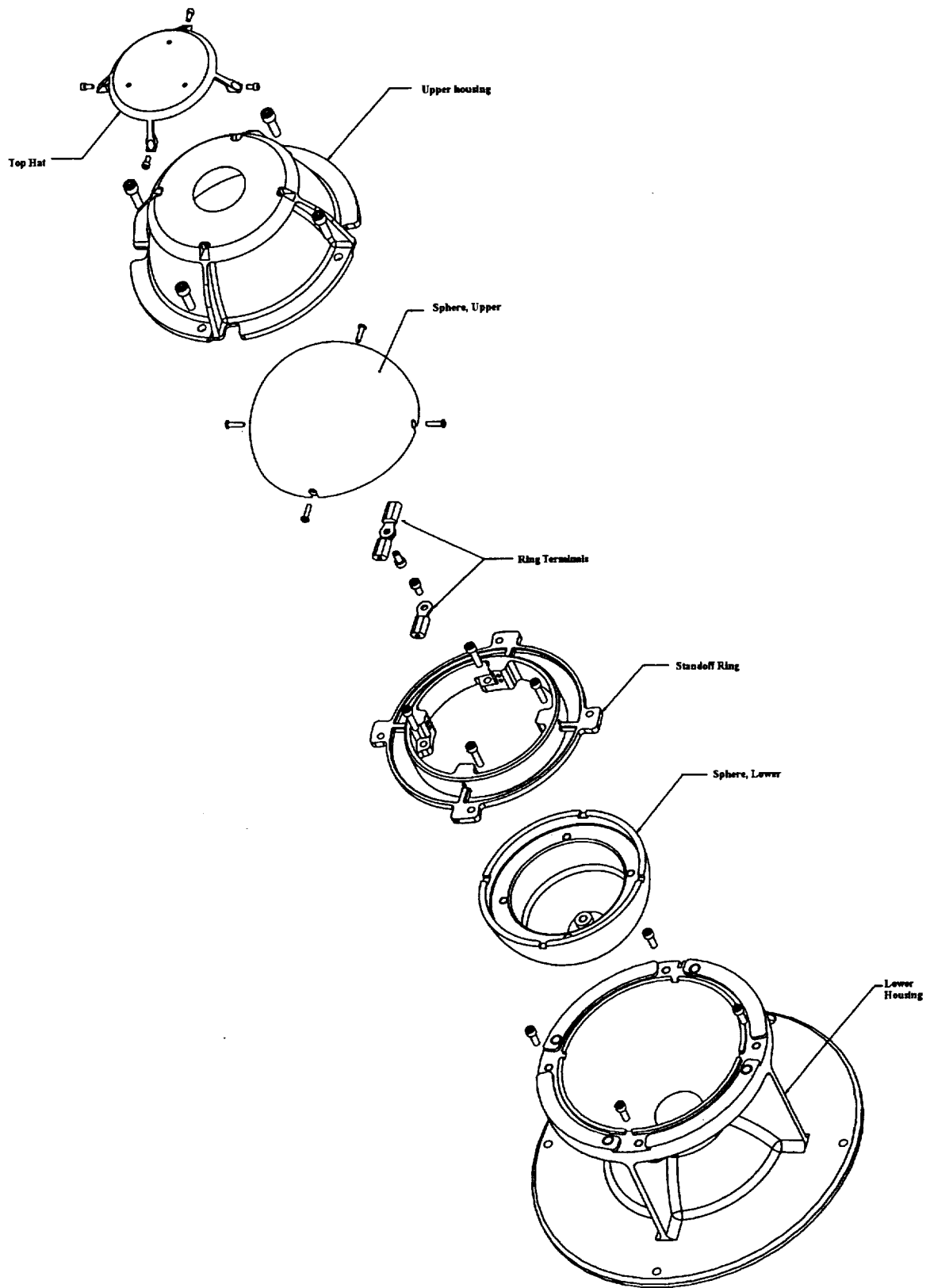


Figure 2. Exploded view of the upper deflection system.

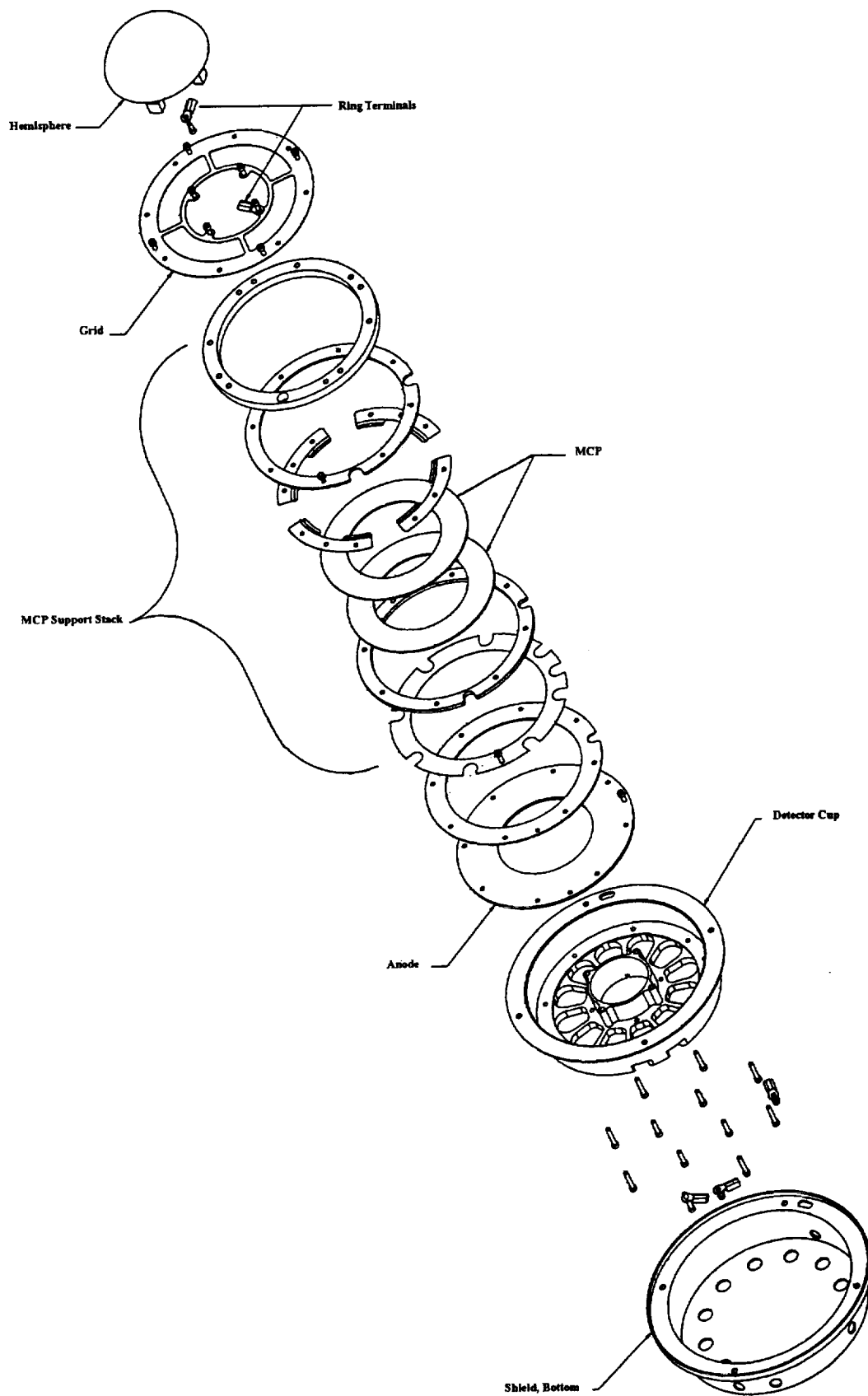


Figure 3. Exploded view of the lower deflection and sensor systems.

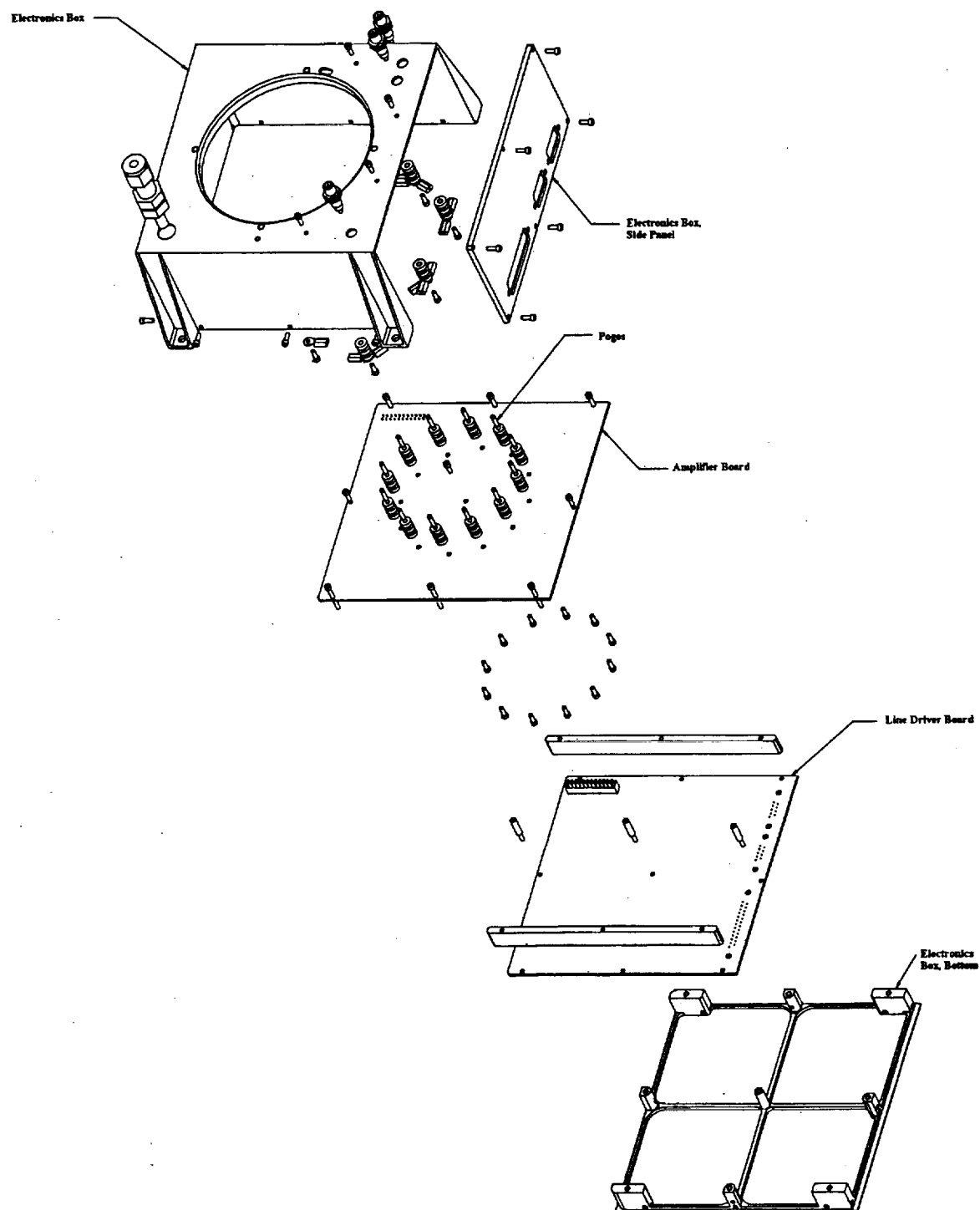


Figure 4. Exploded view of the electronics box.

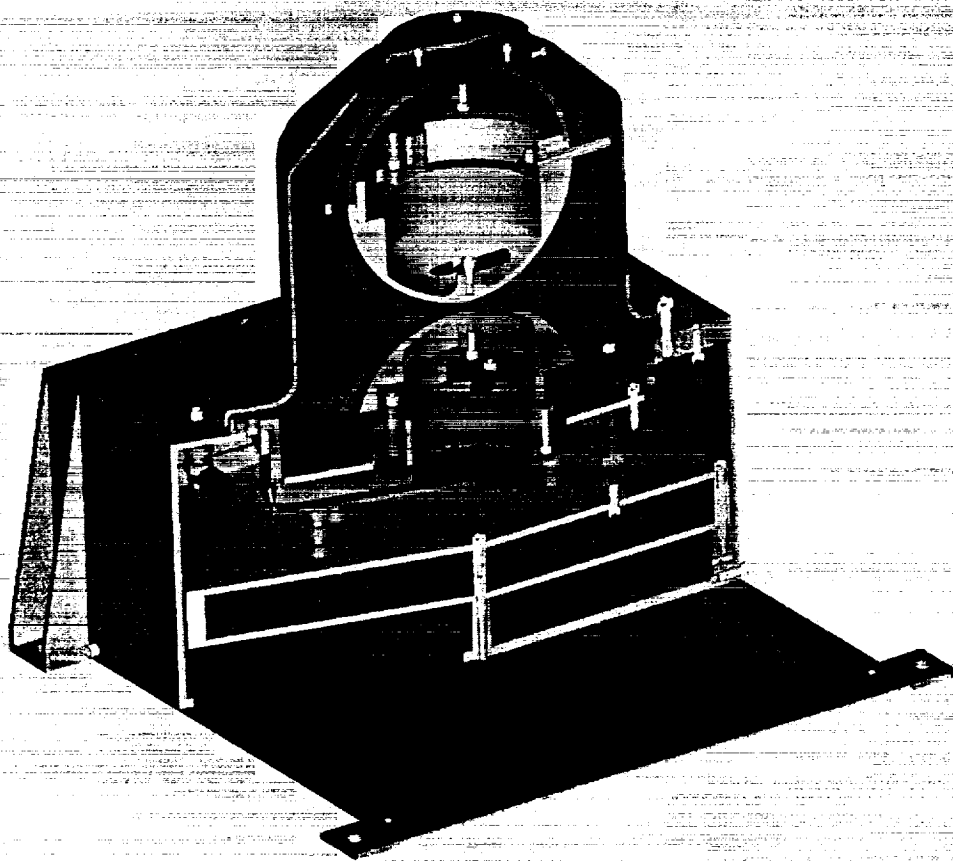


Figure 5. Cut away view of the 270° top hat analyzer on top of the laboratory electronics box.

Flat Field

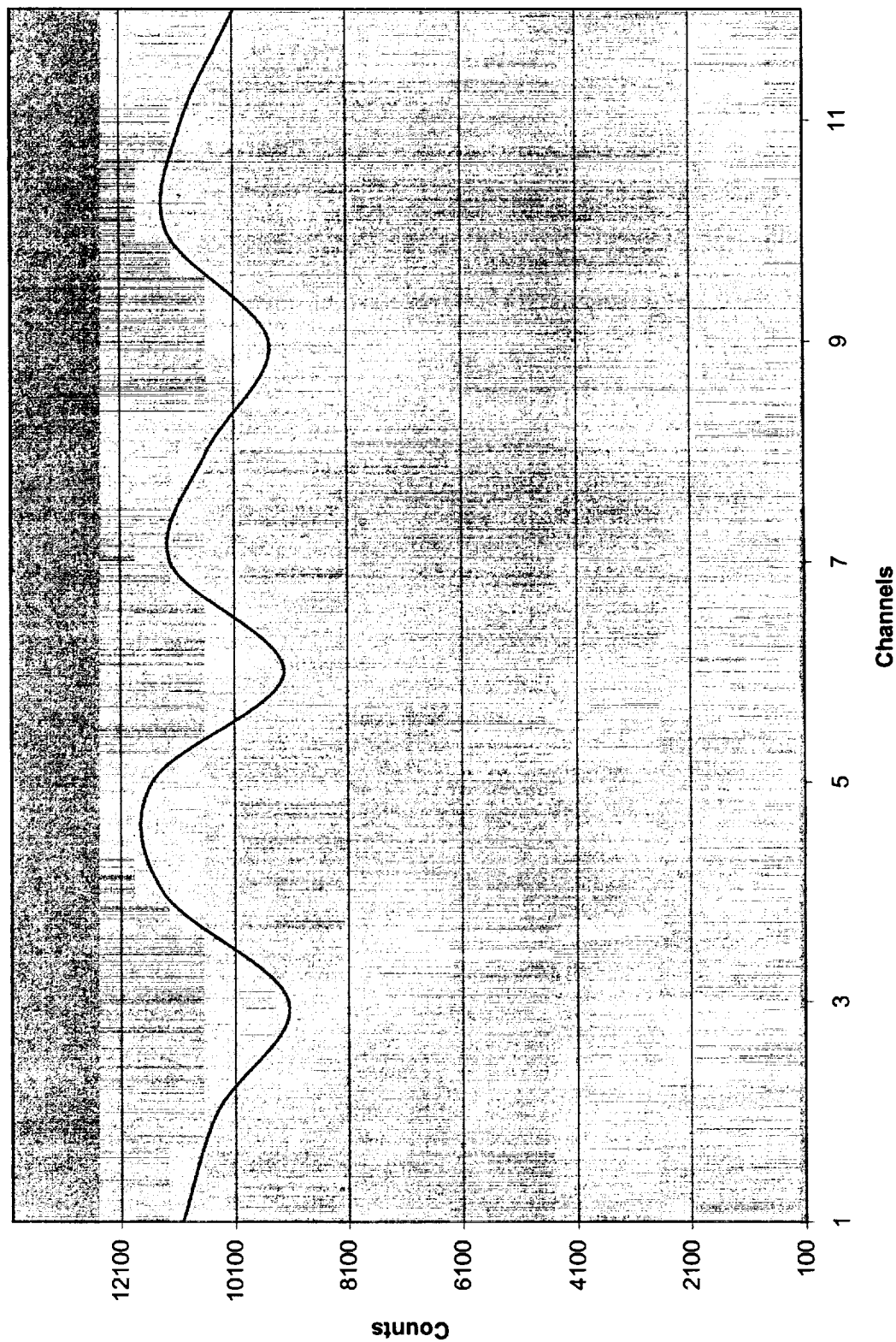


Figure 6. UV Flood test of the 270° top hat analyzer showing influences in sectors 3, 6, 9, and 12.

manufacture. Since this was not a flight program, but a laboratory test system, a lesser quality MCP was used to reduce program costs (see proposal). This test shows a non-zero dark count across the MCP and the amplitude of this dark count is anode dependent.

Tests of the deflection system occurred in the first characterization task. A lower energy electron beam was used. The beam is generated by a Kimball Physics flood gun. The profile of the test electron beam is shown in Figure 8. During the first characterization, the mu-metal shield was removed and the internal deflection system was uncoated with Ebanol-C (used to absorb secondary electrons within the deflection system). Since there is no mu-metal shield on the unit for this test, it is anticipated that there will be a strong influence during deflection due to the Earth's magnetic field (see deflection calculations in proposal), and passage of low-energy electrons would not occur. Therefore, beam energies were kept toward the higher limits of the electron gun for this test.

Since the instrument is uncoated for secondary electron absorption, it is anticipated that the background counts would be about 10% for an uncoated instrument of a good design. Instruments are known to achieve a 5% background by coating with aerodag (graphite) as an inexpensive solution and in the 1%-2% range for instruments coated with a gold-black absorbing surface (the expensive solution). Due to the properties of gold-black, the Ebanol-C solution seems the most appropriate coating for absorbing secondary electrons generated internally within the 270° instrument. Thus, the 10% background solution is the appropriate value to use as a metric for this test.

The instrument was activated in an electron beam on 1 keV. There was 2000 volts placed across the MCP to activate the sensor. A quick scan of the deflection plate voltage (Figure 9) showed a peak at about 160 volts, which gives an analyzer constant of about ($k = 1000 \text{ keV} / 160 \text{ V}$) 6.25. The peak was about 110,000 counts and the width at half maximum is about 1.4 volts, giving an energy resolution of about 1.3%. Note that the resolution of this plot is not very well determined because of the coarse data resolution, but it does show that the energy resolution is within the correct range. Since the energy resolution needs to be explored in more detail, later tests are designed where there is a greater data resolution so that the energy resolution can be investigated accurately. The purpose here is to find an appropriate deflection voltage setting for which to use when doing an azimuth scan. Thus, a larger voltage sweep was used to find the peak deflection value.

When a 1 keV electron beam is exposed to the instrument and the instrument is rotated in azimuth, Figure 10 results. For this test, the 270° top hat deflection voltage is set to 159 volts, at the peak of the distribution (from Figure 9). The anode response is fairly flat on those anodes that do not contain standoffs to block the electrons and a drastic signal cavity is shown at the location of the standoffs for those anodes containing their influence. In the center of this figure is displayed the data from an anode which contains blockage due to a standoff (channel 9). Just before the standoff influence, there is a decrease in the intensity of the electron beam and then a slight increase in count at the edge of the standoff. Under the influence of the standoff, the normal background decreases from the normal 2.5% - 4% of the peak count to 0.05% - 0.25% of the peak count indicating that the standoffs are an efficient blockage to the electron beam.

Figure 11 shows the theoretical response functions of the 270° top hat analyzer from the proposal. Both the elevation and energy response curves of the 270° instrument show rounded peaks, so we should not expect curves resulting from laboratory measurements to be sharply peaked. In addition, the theoretical response functions indicate asymmetric distributions. For the elevation response shown in Figure 11A, the elevation peak is about 2.5° from normal incidence (at 90°). The asymmetry shows that the steeper side of the distribution is toward the side of the distribution which is most off-axis. The energy response shows a steeper distribution at the lower-energy side of the response peak and a shallower distribution at the higher-energy side of the response peak.

The 270° top hat was scanned in elevation and plate voltage at a beam energy of 1 keV in order to reproduce instrument response functions. The MCP acceleration voltage was 2000 volts. This elevation-energy (deflection voltage) matrix was examined to generate the elevation response at all energies (Figure 12) and the voltage response at all elevations (Figure 13) for the anode at 2.5° azimuth (channel 10). Examining the elevation response, we see that the peak is shifted toward one side of normal incidence (the positive side of 0° in this figure). The elevation response is sharper on the side of the peak shift, which is consistent with the theoretical response curve. The peak of the response function is shifted by about 2.4° compared to the 2.75° theoretical value. The half width is 2.8° compared to the 3.5° theoretical value.

The deflection voltage response also approximates the theoretical curve; however the theoretical shape tends toward a thinner peak and broader wings than the measurements show. The distribution peak is at 160 volts and the

Dark Counts

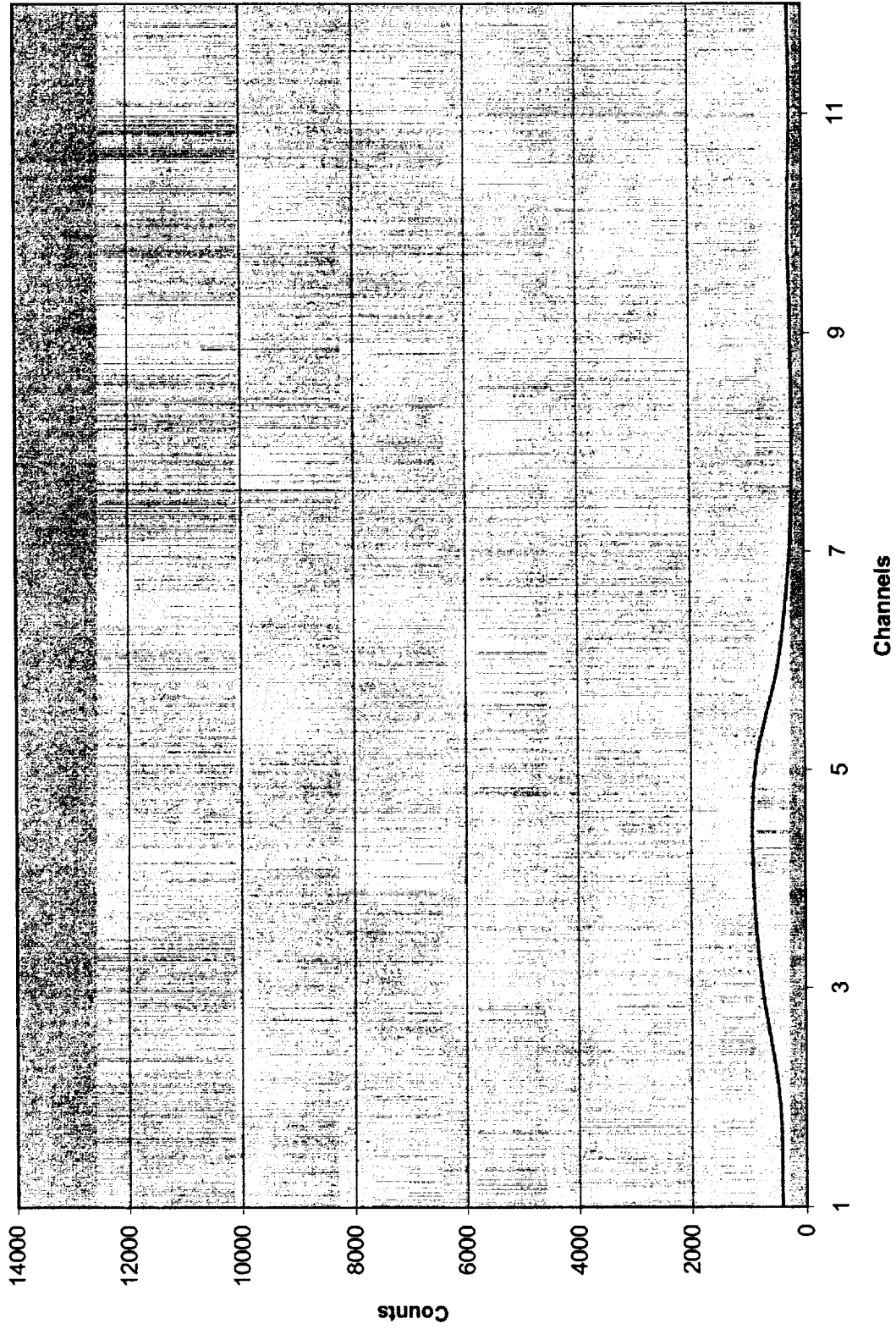
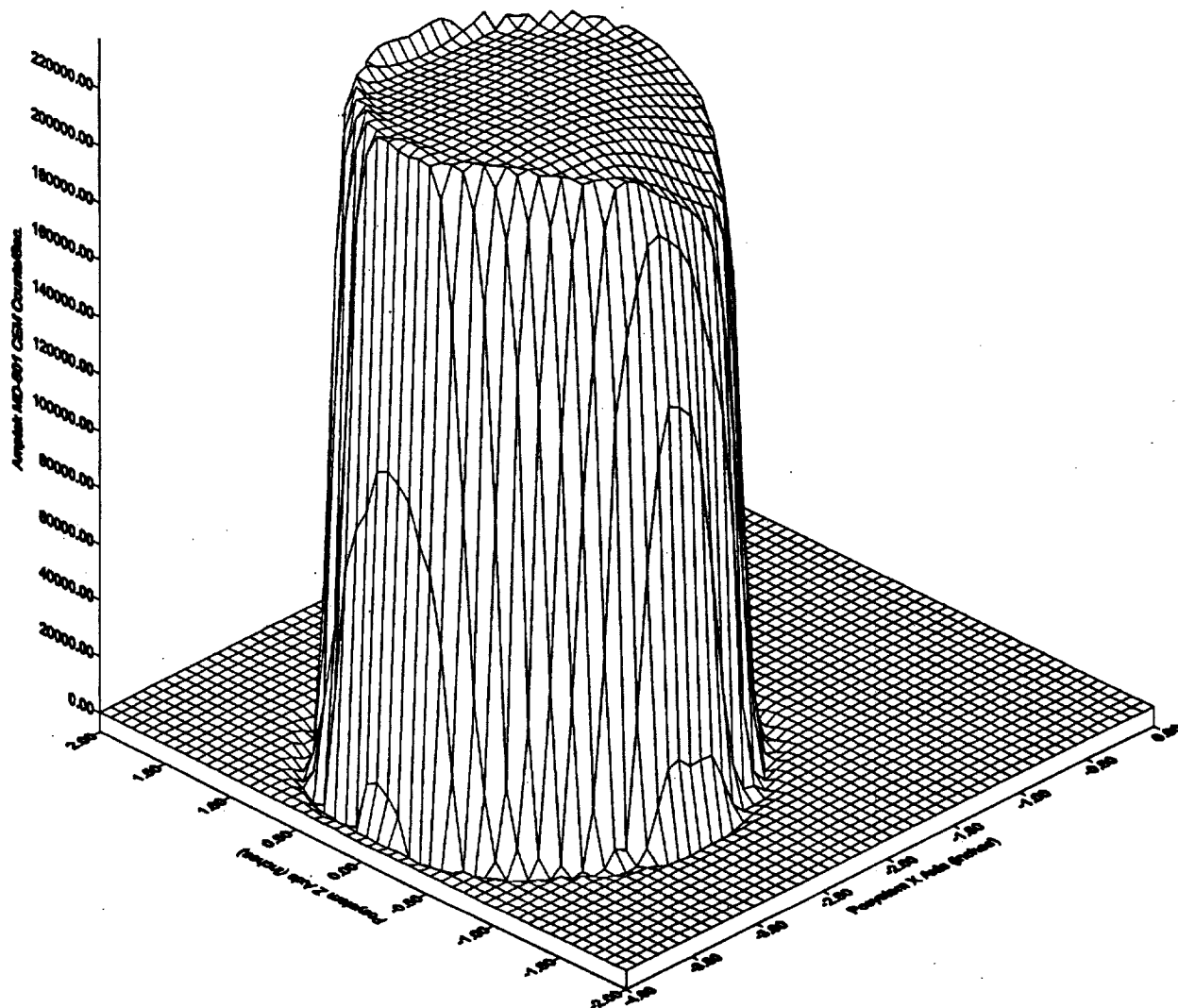


Figure 7. Background MCP detection system test.



Kimball Physics FRA-2X1-2 Electron Source
 uMetal Collimator, 10mm Aperture
 Amplek MD-501 Detector with 1mm Aperture
 500eV, 1.2A @ 0.95V, +10V Grid.
 13 November, 2000 PS13NOV085327.dat

Figure 8. Electron beam profile.

1000eV, 2000V, El:0 deg, Az:0 deg, X:0", Z:-0.75"

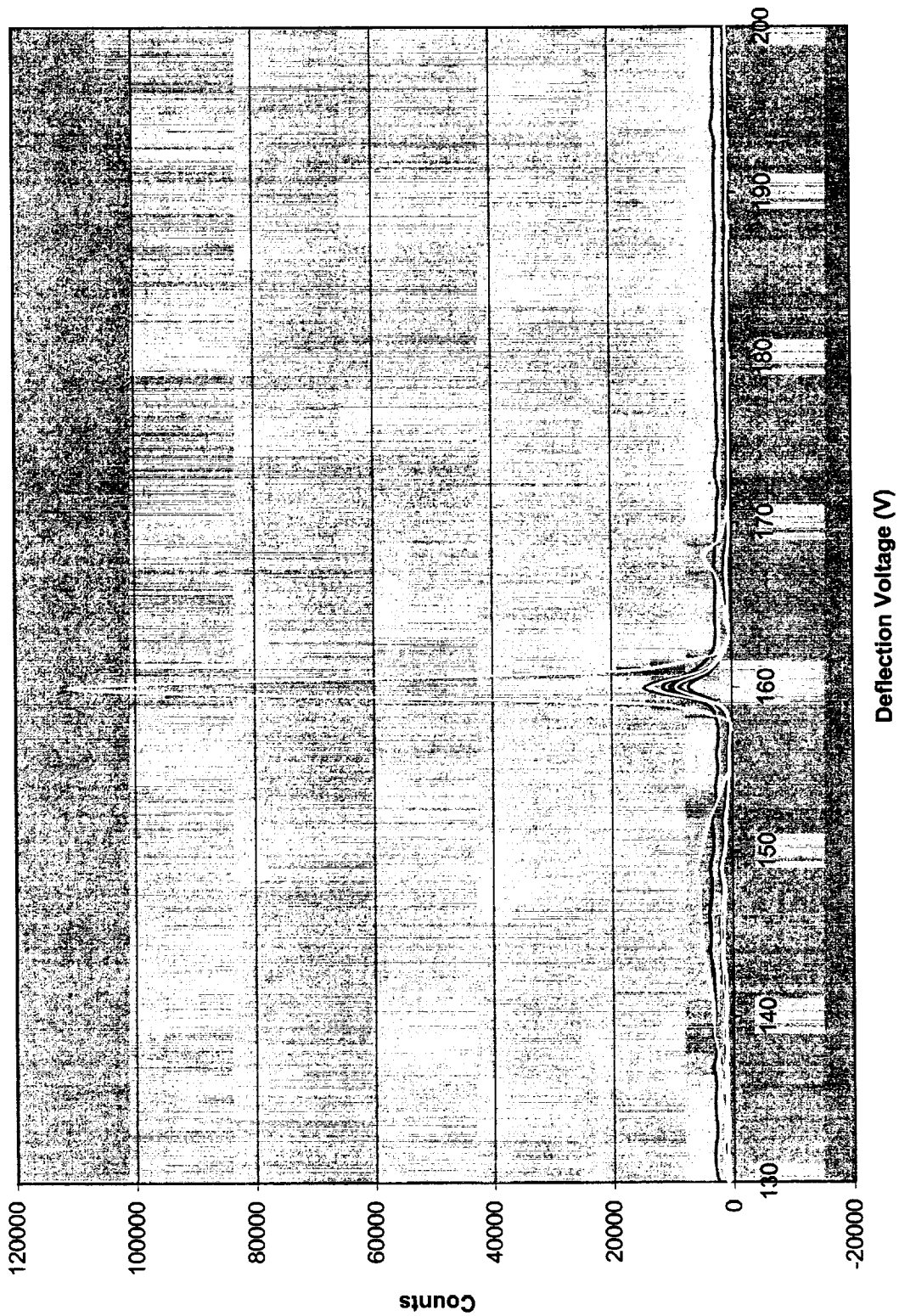
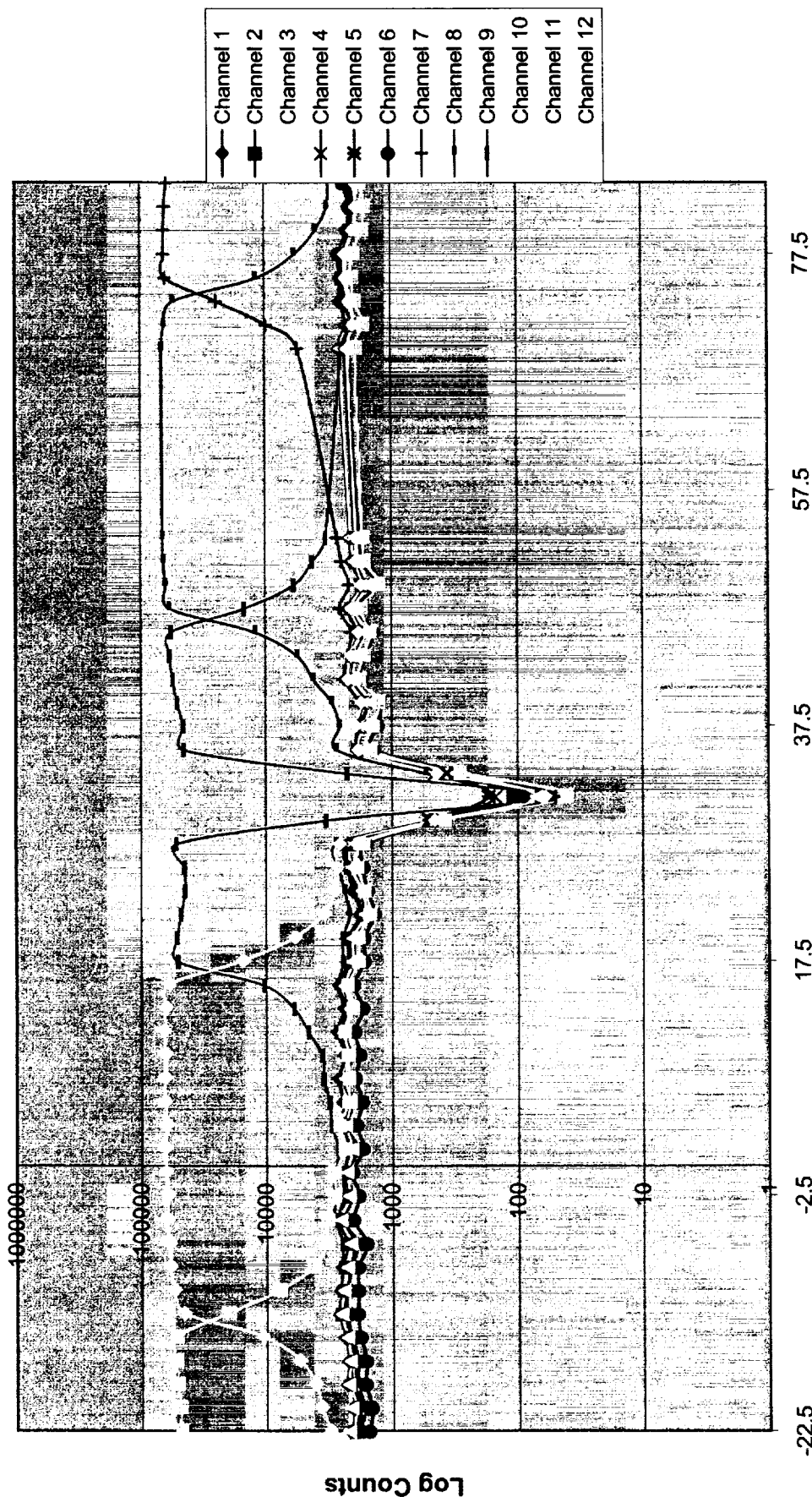


Figure 9. Quick deflection voltage scan.

Azimuth Scan (1000eV, El:2.5 deg, X:0", Z:-0.75", Defl. Voltage:159V)



Azimuth Angle (Degrees)

Figure 10. Azimuth scan of the 270° top hat.

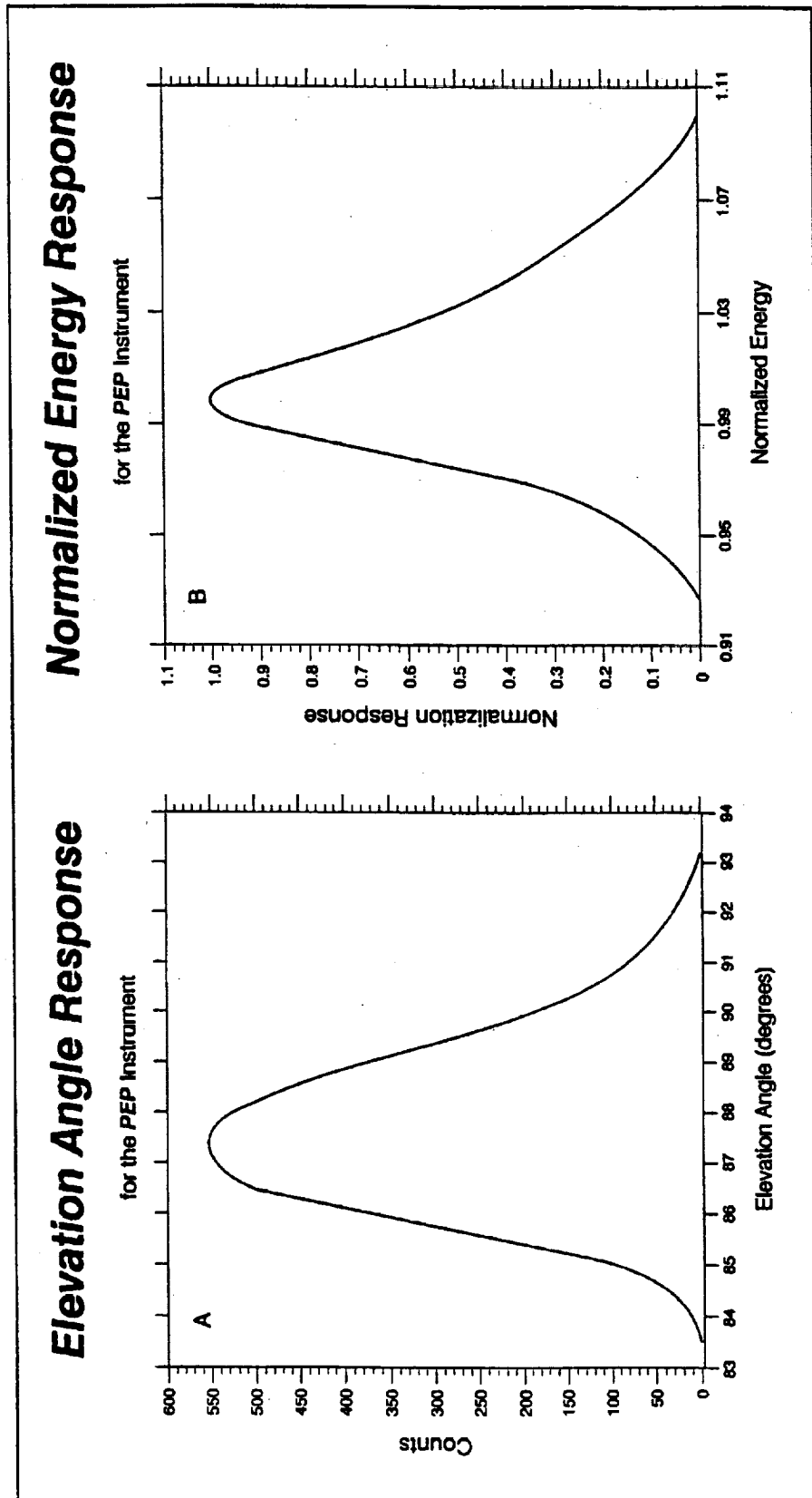
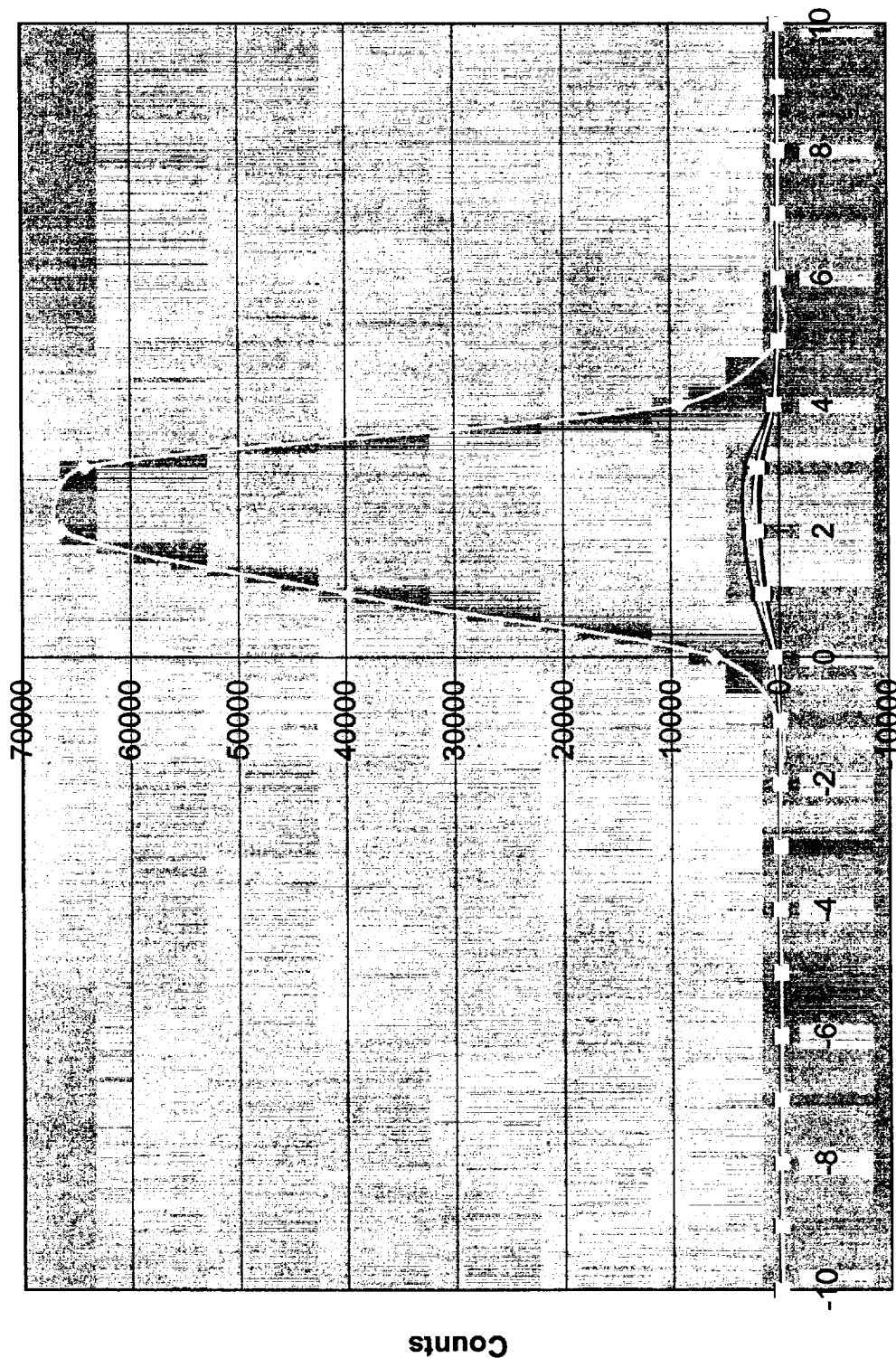


Figure 11. Theoretical response of the 270° top hat. A. Elevation angle response. B. Normalized energy response.

Elevation Scan (1000eV, Az:2.5 deg, X:0", Z:-0.75", Defl. Voltage:159V)



Elevation Angle (Degrees)

Figure 12. Measured elevation response from channel 10.

half width is 5.25 volts, giving a measured resolution of 3.2% (the theoretical resolution from Table 1 is 5.7%). It is possible that the energy resolution is smaller than the theoretical value since we know that the outer diameter of the upper hemisphere of the lower housing is a few thousands of an inch too small. This would increase the internal electric field causing the distribution to be shifted toward higher electron energies and narrowing the energy range of acceptance to the 270° analyzer.

4. Currently In Process

The 270° analyzer is currently under modification. The instrument is beginning the phase of coating internal deflection systems. The Ebanol-C coating was to be performed by Los Alamos using a method developed for the cusp ion detector (CID) and cusp electron detector (CED), both top hat style instruments, of the Svalbard Rocket Campaign; however, arrangements have not been able to be made. Other manufactures were contacted to supply internal coatings, but their costs were found to be well above the amount which could be afforded by this project. The original SwRI cost was prohibitive, also; however, SwRI arranged to subsidize coating costs so that it is affordable by this project. Internal coatings of Ebanol-C will now be performed by SwRI.

5. Remaining from Year 2

Final assembly and characterization of the instrument was to occur in year 2. Five anodes for characterization were to be chosen as follows: (1) the least obstructed deflection path, (2) the most obstructed deflection path furthest from the inner sphere electrical connection, (3) the most obstructed deflection path containing the inner sphere electrical connection, (4) the anode with the least obstructed deflection path which is near the mirror image of (1), (5) the most obstructed deflection path furthest from the inner sphere electrical connection which is near the mirror image of (2). Design errors have lead to changes between anodes containing standoffs and those which do not. With the developed accumulation system, all anodes will be monitored simultaneously during testing so that their results can be compared and contrasted.

Experiments were designed in four separate phases, 1-4, conducted at an energy of about 1 keV so that differences could be highlighted and a detailed understanding of instrument workings could be accomplished:

- Raw, Uncoated Analyzer,
- Raw, Uncoated, Magnetically Shielded Analyzer,
- Blackened Analyzer,
- Blackened, Magnetically Shielded Analyzer.

These characterization tests have been changed due to budgetary influences. The first test was concluded during Year 2 and characterization phases 2-3 will no longer be performed. The last phase, 4 (blackened, magnetically shielded analyzer), will be conducted with the remaining funds. At this point, blackening of internal parts will be accomplished and the instrument model will be reassembled with the magnetic shield. This will be the final instrument configuration. The Ebanol-C black coating will reduce the background noise level of secondary emitted electrons in the deflection region. The mu-metal shield will allow lower energy electrons to be deflected.

Due to unavailability of the electron chamber used in the tests described during phase 1, the 270° top hat instrument testing has been forced to use another testing facility. In this system, it is not possible to remount the flood gun (which was used during phase 1 testing) because of the additional cost of engineering a solution for the new system. Mounting the flood gun in the orientation necessary for the new vacuum system is unaffordable by this project. Future testing of the 270° instrument will need to occur at beam energies greater than anticipated due to the type of electron gun already mounted in the new vacuum system. Beam fluxes will be energy dependent and beam energies below 1 keV will most likely not contain enough flux to adequately test the instrument.

New cables and mounting hardware will have to be manufactured for the new vacuum system. Most of the mounting hardware is not compatible with the system which was in-use for testing the uncoated analyzer. In addition, the data accumulation system will need to be integrated into the control system for the new chamber.

Energy:1000eV, MCP:2000V, El:2.5 deg, Az:2.5 deg, X:0", Z:-0.75"

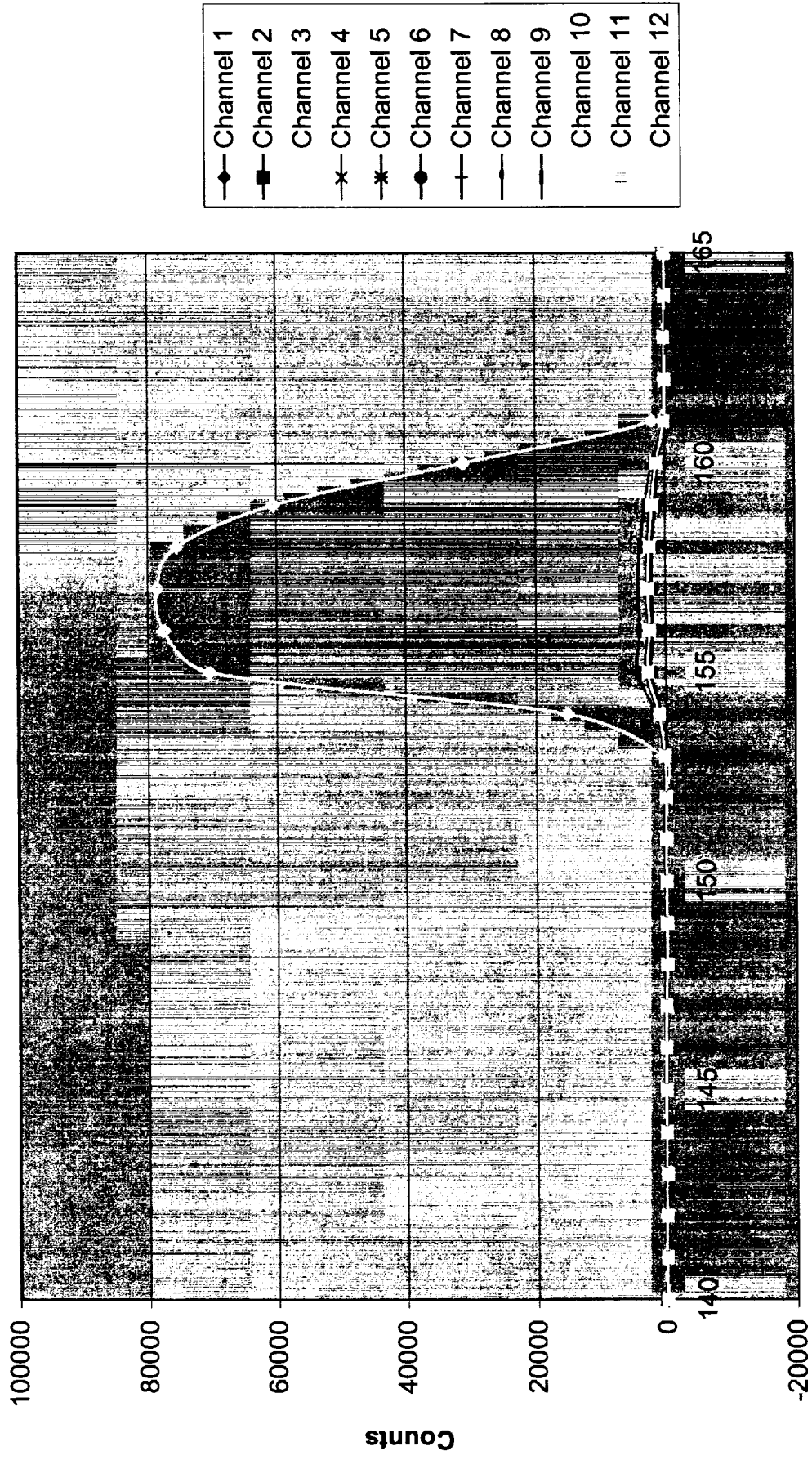


Figure 13. Measured deflection voltage response from channel 10.

6. Schedule

The schedule has been adjusted to reflect the current status of this project. It is presented in Table 2.

7. Budgets

The second year award value was taxed at 5.8% by NASA. There has been an adjustment in personnel working on this project in order to attempt a labor savings to allow the accomplishment of most of the tasks described by the original proposal. Note that unanticipated events have forced removal of testing characterization phases 2 and 3 from this project. In addition, the loss of a test system has forced a request for a time extension. This time extension was discussed with the PIDDP program scientist and granted.

8. Acknowledged Major Staff

Major staff members who are working on this project or who have worked on this project during time covered by this report, besides the authors, are as follows: J. R. Scherrer — mechanical, S. E. Weidner — electrical, S. E. Pope — mechanical, J. Langle — mechanical, and L. Björk — consultant. All have contributed their talents and expertise to this project.

9. References

Winningham, J. D., D. T. Decker, J. U. Kozyra, J. R. Jasperse, and A. F. Nagy, "Energetic (>60 eV) Photoelectrons," *J. Geophys. Res.*, **94**, 15335, 1989.

Table 2: Updated Project Time Line

Work Task	Year 1												Year 2												Extension											
	1999						2000						2000						2001						2001											
	J	J	A	S	O	N	D	J	F	M	A	M	J	J	A	S	O	N	D	J	F	M	A	M	J	J	A	S	O	N						
Physical Instrument																																				
(a) Drawing																																				
(b) Purchase Metal																																				
(c) Machining																																				
(d) Assembly																																				
(e) Blacking (Ebanol c)																																				
(f) Electrical Connection																																				
MuMetal Shield																																				
(a) Drawing																																				
(b) Purchase Metal Can																																				
(c) Assembly																																				
Board 1: MCP Sensor Board																																				
(a) Drawing																																				
(b) Purchase Parts																																				
(c) Build																																				
(d) Test																																				
Board 2: Amplifier Board																																				
(a) Drawing																																				
(b) Purchase Parts																																				
(c) Build																																				
(d) Test																																				
Board 3: Line Driver Board																																				
(a) Drawing																																				
(b) Purchase Parts																																				
(c) Build																																				
(d) Test																																				
Instrument Characterization																																				
(a) Initial Fitting																																				
(b) Characterization 1																																				
(c) *Shield Installation																																				
(d) *Characterization 2																																				
(e) Black Assembly																																				
(f) *Characterization 3																																				
(g) Shield Installation																																				
(h) Characterization 4																																				
Reporting																																				
(a) Year End Report																																				
(b) Final Report																																				

* Characterization Test Removed due to Budgetary Constraints